# Ion-Solvation Reactions of Phosphine

**J. W. Long and J. L. Franklin***

*Contribution from the Department of Chemistry, Rice University, Houston, Texas 77001.* *Received September 5, 1973*

**Abstract:** A study of the ion–molecule reactions of phosphine observed in a drift tube ion source reveals two different sets of product ions at elevated source pressures. At a source temperature above 25° $PH_4^+$ is formed as the major ion by primary ion reactions. $PH_4^+$ then reacts further with phosphine by a solvation equilibrium reaction followed by dissociation. The ions formed in this manner are $P_2H_5^+$, $P_3H_6^+$, and $P_4H_7^+$. The activation energy for the forward and reverse dissociation from the equilibrium product was measured. At source temperatures below 25°, ions are observed which have the general formula $R^+(PH_3)_n$ where $R^+ = PH_4^+$, $P_2H_5^+$, $P_3H_6^+$, and $P_4H_7^+$. These ions constitute four solvation series. Where $R^+ = PH_4$, $n = 0$–6 was observed, and from the measured equilibrium constants thermochemical data for successive solvation steps were obtained. A calculation of the electrostatic forces contributing to the total potential energy for the $PH_4^+ \cdot PH_3$ interaction was done. The low values for the free energy and enthalpy of solvation for phosphine compared to ammonia are explained on the basis of the small dipole and large radius of the phosphine solvent. The entropy for the first solvation is calculated and the change in entropy with solvation is discussed.

During the development of a new drift tube high-pressure ion source in this laboratory we chose to study the solvation reactions of ammonia to characterize the performance of the new source. The thermochemical data obtained agreed with previous data reported for the solvation of $NH_4^+$ in ammonia.[1] After establishing that equilibrium solvation reactions could be studied in the new source, we decided it would be instructive to investigate the reactions of the second hydride in the group V series, phosphine.

Although phosphine is a congener of ammonia, one might expect considerably different results in the study of the solvation reactions of $PH_4^+$ in phosphine due to the larger molecular diameter and small dipole moment of the compound. We undertook the study of the solvation of $PH_4^+$ in phosphine to obtain thermochemical data for this nearly nonpolar system to compare the results with the thermochemical data available for the polar ammonia system.

Several investigations of the ion–molecule reactions of phosphine have been done at relatively low pressures and constant ambient temperatures.[2–5] Under these conditions, the major product ion formed is the protonated phosphine ion, $PH_4^+$, which comprises more than 90% of the total product ion intensity. Other product ions containing more than one phosphorus atom were observed as minor constituents.

In this paper, the ion–molecule reactions of phosphine have been studied at elevated source pressures and over a wide temperature range. An extensive set of reaction products which have not been reported previously was obtained under these conditions. The reaction mechanism for the production of the new set of product ions and some kinetic parameters are presented.

## Experimental Section

A description of the drift tube ion source and its operation has been given previously and only a summary of the operational parameters is given here.[1] The ion source has a reaction path length of 5.5 cm. A 2 V/cm field gradient applied to the metal rings inside the source induces ions formed by electron impact to drift through the source at pressures in the 1-Torr region. The ions exit the source at ground potential and are detected by a quadrupole mass filter.

Heater probes allow operation up to 180°. The source is jacketed so that a low-temperature solution can be circulated around the drift tube walls. Ethanol, used as the coolant, is circulated through a large coil in a slush bath and then through the source jacket. Different temperature ranges were obtained by changing the chemical composition of the slush bath. The drift tube wall temperature is detected by a Pt–Pt thermocouple probe imbedded in the wall near the ion exit plate. The probe detects the wall temperature over the range ±200° with an error of ±4°.

Research grade phosphine (Matheson) was used as purchased without further purification. Low-pressure electron impact spectra indicated no detectable impurities. The gas was introduced into the drift source from a 2-l. bulb on a high-vacuum manifold. With the correct variable leak adjustment, pressure studies at 1-Torr pressure could be conducted over an extended period of time with a minimal variation in the source pressure. The source pressure was detected by a capacitance manometer connected directly to the drift tube through large bore tubing.

In the study of the low-pressure ion–molecule reactions of phosphine, the backing plate was kept at +6 V and the field gradient was set at 2 V/cm. This backing plate voltage setting gives reproducible kinetic results for gases at low pressures but has no effect on the product distribution at pressures above 0.10 Torr. Low-pressure studies were done at 150 eV energy while high-pressure analyses were done at 400 eV electron energy. The only effect the higher electron energy had on the product ion distribution was to increase the over-all ion intensity recorded.

## Results

A low-pressure analysis of the primary ion reactions of phosphine was done at 160°, a temperature at which the reaction to higher order products was minimized.

In Figure 1 the relative intensities of the primary reactant ions and low-pressure product ions are plotted against the phosphine pressure. $PH_3^+$ appears to increase initially and then above 2 or 3 $\mu$ decreases rapidly. Presumably the initial rise is due to charge exchange with $P^+$ and $PH^+$ both of which are energetically capable of exchanging with $PH_3$. On the other hand, $PH_2^+$ is not capable of exchanging with $PH_3$. The primary ions react rapidly through multiple channels to form the various products.[2–5] A rate constant calculated from the slope of the logarithm of the primary ion intensity against the phosphine pressure

(1) J. W. Long and J. L. Franklin, *Int. J. Mass Spectrom. Ion Phys.*, in press.
(2) M. Halmann and I. Platzner, *J. Phys. Chem.*, 71, 4522 (1967).
(3) D. Holtz and J. L. Beauchamp, *J. Amer. Chem. Soc.*, 91, 5913 (1969).
(4) J. R. Eyler, *Inorg. Chem.*, 9, 981 (1970).
(5) D. Holtz, J. L. Beauchamp, and J. R. Eyler, *J. Amer. Chem. Soc.*, 92, 7045 (1970).

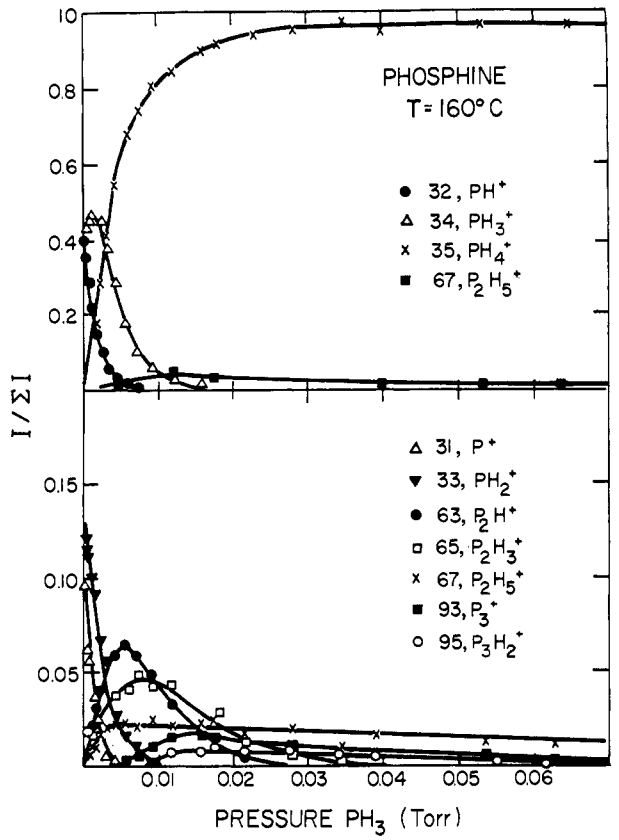


Figure 1. Primary and secondary ion reactions at low pressure, $T = 160°$. Relative ion intensity *vs.* phosphine pressure (in Torr).

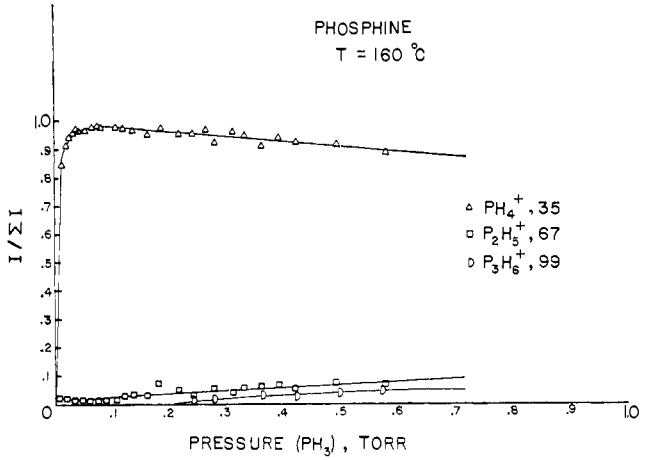


Figure 2. Product ion distribution at high pressure, $T = 160°$. Relative ion intensity *vs.* phosphine pressure (in Torr).

corresponds to the total rate constant for reaction of the primary ion through all possible channels.

$PH_3^+$ has been shown to react with $PH_3$ by one channel only, producing $PH_4^+$ by proton transfer. The rate constant we obtained for this reaction, $9.2 \times 10^{-10}$ cm³/(molecule sec), is in good agreement with the literature.[5] The reaction time was calculated from the free-fall time for ions to traverse the source. This is a good approximation at low pressures.

Our source is not well suited to the separation and measurement of the rates of individual reactions from a complex such as occurs with phosphine. However, the rates of decay of the various primary ions can be determined from the usual semilog plot where the slope gives the sum of the rate constants for all of the reactions of the primary ion in question. These over-all decay rates are given in Table I along with values by Holtz, Beauchamp, and Eyler[5] and by Halmann and Platzner[2] for comparison. The agreement of the rate constants for reactions of ions other than $PH_3^+$ is only approximate but perhaps is as good as might be expected for the wide difference in the methods and apparatus used. Our measurements were made at both 60 and 160° with generally good agreement.

The product ions formed fall into two types. As seen in Figure 1, the product ions *m/e* 63, 65, 93, and 95 react further to form $PH_4^+$ at higher pressures. A second set of product ions *m/e* 67 and 99 do not disappear but are formed from $PH_4^+$ at higher pressures and will be discussed in the next section. The rate of formation of $PH_4^+$ is very rapid and this ion is formed as the major product ion (relative intensity of 0.98) at pressures greater than 0.030 Torr.

The observed reactions at low pressures are consistent with those previously reported.[3-5] The low-pressure primary and secondary ion reactions occur rapidly and do not interfere with the reactions observed at higher pressures.

Holtz, *et al.*,[5] have shown that $P_2H^+$ arises almost entirely from $P^+$ and $PH_2^+$ both of which disappear at about the pressure at which $P_2H^+$ also begins to decrease in intensity. Since no $P_2H^+$ is formed above that pressure, a semilog plot of the declining portion of the $P_2H^+$ curve will give the rate constant for the disappearance of $P_2H^+$, presumably by the reaction

$$P_2H^+ + PH_3 \longrightarrow PH_4^+ + P_2$$

Similarly, $P_2H_3^+$ is formed from $PH^+$ and $PH_2^+$ and it decays after the primaries are essentially gone. Thus, the rate constant for the reaction

$$P_2H_3^+ + PH_3 \longrightarrow PH_4^+ + P_2H_2$$

can be determined in a manner similar to that employed with $P_2H^+$. The results are included in Table I.

Table I. Rate of Decay of Ions in $PH_3$ (cm³/molecule sec)

| | $10^{10}k$ | | | |
|---|---|---|---|---|
| | This study | | Holtz, | Halmann and |
| Ion | 160° | 60° | *et al.*[a] | Platzner[b] |
| $PH_3^+$ | 9.2 | 12.4 | 10.8 | 9.8 |
| $PH_2^+$ | 11.4 | 15.6 | 8.4 | |
| $PH^+$ | 19.7 | 21.0 | 9.3 | |
| $P^+$ | 20 | 20.0 | 8.2 | |
| $P_2H_3^+$ | 3 | | | |
| $P_2H^+$ | 4.1 | | | |

[a] Reference 5. [b] Reference 2.

Extending the analysis at 160° to higher pressures one observes the product ion distribution given in Figure 2. Above 0.050 Torr the $PH_4^+$ ion intensity begins to drop slowly and $P_2H_5^+$ to appear in small intensity. We think this behavior is best explained by an equilibrium reaction to form $P_2H_7^+$ which subsequently dissociates to $P_2H_5^+$ in accordance with (1). It is possible that

$$PH_4^+ + PH_3 \underset{k_{-1}}{\overset{k_1}{\rightleftharpoons}} P_2H_7^+ \xrightarrow{k_2} P_2H_5^+ + H_2 \qquad (1)$$

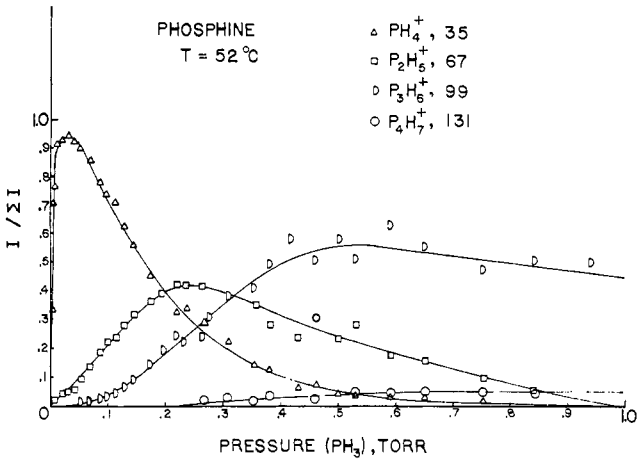


**Figure 3.** Product ion distribution, $T = 52°$. Relative ion intensity *vs.* phosphine pressure (in Torr).

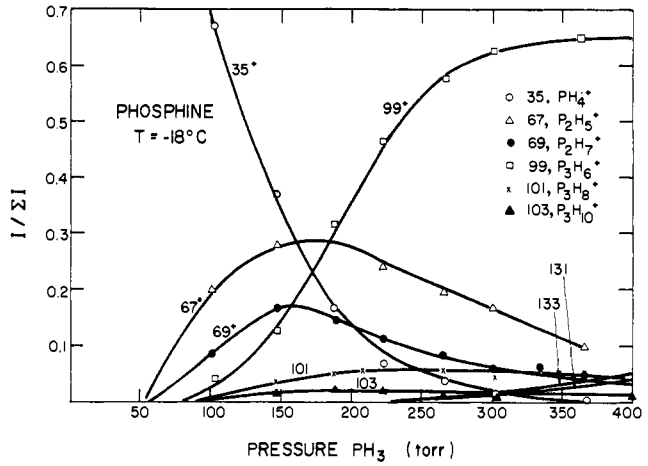


**Figure 4.** Product ion distribution, $T = -18°$. The "intermediate" ions *m/e* 69, 101, and 103 are observed. Relative ion intensity *vs.* phosphine pressure (in Torr).

$P_2H_5^+$ could be formed by transfer of a proton from $PH_4^+$ to $P_2H_4$ present in small amounts as an impurity. We were unable to detect $P_2H_4$ by direct ionization but admittedly this is not a very sensitive test. Conceivably, also, $P_2H_4$ might be formed by reaction on the filament or the ionization chamber surfaces. If so, the formation of $P_2H_4$ would probably be second order in pressure and the formation of $P_2H_5^+$ would thus show a higher order pressure dependence than would be expected from (1) or that was actually observed. Thus, while we cannot be entirely certain, we think the formation of $P_2H_5^+$ probably occurs by reaction 1. On this assumption we find at 160° that the equilibrium lies far to the left so that only a small amount of the intermediate ion is found. The dissociation rate constant, $k_2$, is also temperature dependent and at this temperature is high; therefore, all of the $P_2H_7^+$ intermediate formed dissociates either back to $PH_4^+$ or to the $P_2H_5^+$ product ion. Only a minor amount of $P_2H_5^+$ is observed at this temperature.

$P_2H_5^+$ reacts with phosphine at higher pressures.

$$\underset{67}{P_2H_5^+} + PH_3 \underset{k_{-3}}{\overset{k_3}{\rightleftharpoons}} \underset{101}{P_3H_8^+} \xrightarrow{k_4} \underset{99}{P_3H_6^+} + H_2 \qquad (2)$$

Again, the $P_3H_8^+$ intermediate rapidly dissociates to $P_2H_5^+$ and $P_3H_6^+$, but only a minor amount of $P_3H_6^+$ is formed.

As the temperature is decreased the equilibrium reaction shifts toward the right and in Figure 3, at $T = 52°$, it is seen that $PH_4^+$ reacts extensively, $P_2H_5^+$ passes through a maximum, and $P_3H_6^+$ is formed as the major product ion at higher pressures. A higher molecular weight product, $P_4H_7^+$, observed at this temperature, is formed by the reaction sequence

$$\underset{99}{P_3H_6^+} + PH_3 \underset{k_{-5}}{\overset{k_5}{\rightleftharpoons}} \underset{133}{P_4H_9^+} \xrightarrow{k_6} \underset{131}{P_4H_7^+} + H_2 \qquad (3)$$

Reactions 1, 2, and 3 given above are in agreement with the ion product distribution observed above ambient temperatures. $k_{-1}, k_{-3}, k_{-5}, k_2, k_4$, and $k_6$ are all large at these temperatures and the intermediate ions are not observed.

When the temperature is decreased below 25° the rates of dissociation of the intermediate ions in either direction become smaller and the intermediate ions are observed in the spectrum. In Figure 4, at $T = -18°$, the intermediate ions *m/e* 69, 101, and 133 appear. At lower temperatures where the intermediate ions are stable, a new set of product ions appears corresponding in mass to the successive addition of $PH_3$ groups to $PH_4^+$ and to the two dissociation products, $P_2H_5^+$ and $P_3H_6^+$. At $T = -18°$, *m/e* 69 and 103 are formed by the addition reactions

$$\underset{35}{PH_4^+} + PH_3 \rightleftharpoons \underset{69}{PH_4^+ \cdot PH_3} \qquad (4)$$

$$\underset{69}{PH_4^+ \cdot PH_3} + PH_3 \rightleftharpoons \underset{103}{PH_4^+ \cdot 2PH_3} \qquad (5)$$

These addition reactions are equivalent to a solvation reaction in which $PH_4^+$ is solvated by neutral phosphine. The general equation for this reaction is

$$PH_4^+ \cdot (PH_3)_{n-1} + PH_3 \rightleftharpoons PH_4^+ \cdot (PH_3)_n \qquad (6)$$

At the lowest temperature (−77°) studied, the masses observed formed by reaction 6 were *m/e* 35, 69, 103, 137, 171, and 205 which are the $n = 0$ to 5 solvation reactions.

Likewise, for the solvation of $P_2H_5^+$, the general equation is

$$P_2H_5^+ \cdot (PH_3)_{n-1} + PH_3 \rightleftharpoons P_2H_5^+ \cdot (PH_3)_n \qquad (7)$$

and the masses observed at −77° are *m/e* 67, 101, 135, 169, and 203 corresponding to $n = 0$ to 4.

For $P_3H_6^+$, the masses observed at $T = -77°$ are *m/e* 99, 133, 167, and 201 corresponding to $n = 0$ to 3.

A fourth solvation series corresponding to the addition of $PH_3$ groups to the $P_4H_7^+$ ion produced the following ions: *m/e* 131, 165, and 199 where $n = 0$ to 2. This series was of very low intensity at any conditions obtained in our instrument. Recapitulating, at high temperatures a relatively simple spectrum containing the product ions of the dissociation reactions 1, 2, and 3 is observed. As the temperature is decreased, the product ions $PH_4^+$, $P_2H_5^+$, $P_3H_6^+$, and $P_4H_7^+$ react by association of $PH_3$ to give four separate series of solvated ions.

In this paper we have emphasized the solvation reactions of $PH_4^+$ because of the interest in comparing

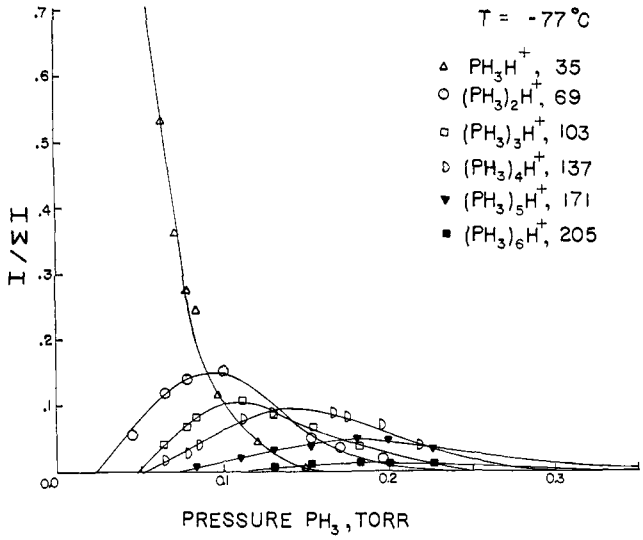


**Figure 5.** Ion distribution for solvation reaction at $T = -77°$: $PH_4^+\cdot(PH_3)_{n-1} + PH_3 \rightleftarrows PH_4^+\cdot(PH_3)_n$. Relative ion intensity *vs.* phosphine pressure (in Torr).

this ion-solvation thermochemistry to the ammonia data. In Figure 5, at $T = -77°$, we see the ion distribution for the successive solvation of $PH_4^+$ as given by the general eq 6.

If reaction 6 comes to equilibrium between successive solvation steps, the equilibrium constant can be written

$$K_{n,n-1} = \frac{I_{PH_4^+\cdot(PH_3)_n}}{I_{PH_4^+\cdot(PH_3)_{n-1}}[P_{PH_3}]} \quad (8)$$

where the $I$'s represent the ion intensities and $P$ is the pressure of phosphine in the source. We have demonstrated previously that valid ion equilibrium measurements can be obtained in the drift tube ion source where the long ion residence times allow ions to come to chemical equilibrium before they are sampled at the ion exit hole.[1] The equilibrium constants for the $PH_4^+$ solvation reactions were analyzed by plotting the right side of eq 8 against the source pressure at constant temperature. As the forward and reverse reactions reach equilibrium, this term should become and remain constant over an extended pressure range. The values for $K_{2,3}$, $K_{3,4}$, and $K_{4,5}$ were obtained from the horizontal portion of the plot shown in Figure 6. Similar curves were obtained at other temperatures and used to determine the successive solvation equilibrium constants of phosphine over an extended temperature range.

van't Hoff plots of the variation in the equilibrium constants with temperature are given in Figure 7. Linear results were obtained for ion clusters from $n = 1$ to 5 over the temperature range +50 to −88°.

**Table II.** Thermochemical Data for Phosphine

$$PH_4^+\cdot(PH_3)_{n-1} + PH_3 \rightleftarrows PH_4^+\cdot(PH_3)_n$$

| $n-1, n$ | $-\Delta G°_{n-1,n}$, kcal/mol | $-\Delta H°_{n-1,n}$, kcal/mol | $-\Delta S°$ (298°K), eu |
|---|---|---|---|
| 0, 1 | 3.7 | 11.5 | 25.9 |
| 1, 2 | 2.5 | 9.2 | 22.3 |
| 2, 3 | 1.8 | 7.3 | 18.4 |
| 3, 4 | 1.7 | 6.2 | 15.0 |
| 4, 5 | 1.6 | 5.5 | 13.2 |

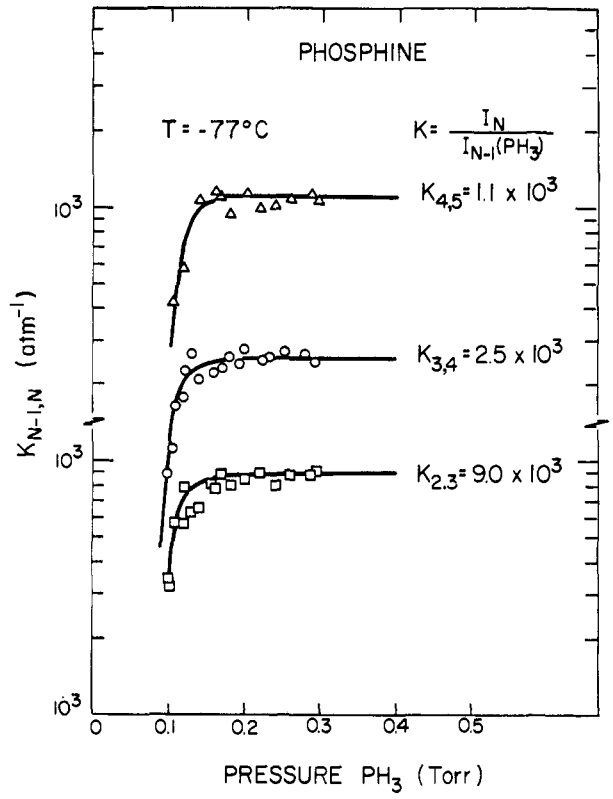


**Figure 6.** Plot of log $k_{n-1,n}$ at constant temperature with the variation in phosphine pressure (Torr). The value of $k_{2,3}$, $k_{3,4}$, and $k_{4,5}$ are taken from the flat portion of the curve.

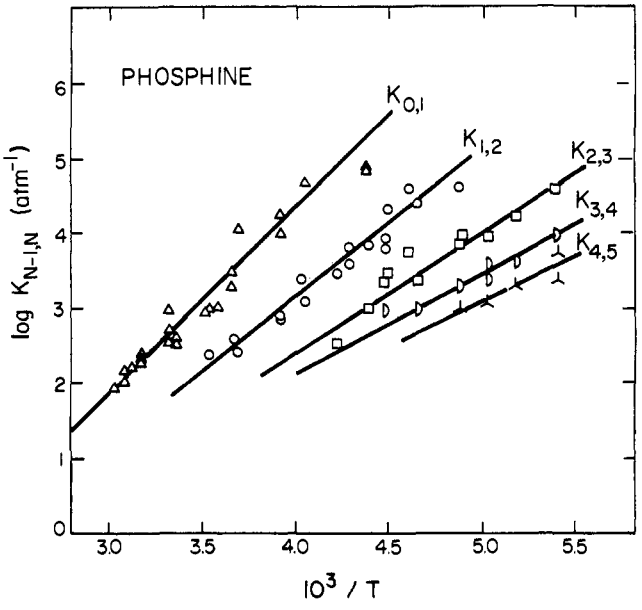


**Figure 7.** van't Hoff plot of the equilibrium constants $n = 0$–5 *vs.* $1/T$(°K). $\Delta H_{n-1,n}$ is obtained from the slope.

Thermochemical data obtained for the solvation of $PH_4^+$ are given in Table II. The free energy of solvation for $n = 0$–5 is calculated at $T = 298$°K and 1 atm of pressure from the equilibrium constant. The heat of solvation is obtained from the slope of the van't Hoff plot and the entropy at standard state is obtained from the difference in enthalpy and free energy of solvation.

As mentioned above, at lower temperatures the sequence of masses 67, 101, 135, and 169 is observed corresponding to the successive addition of $PH_3$ mole-

cules to $P_2H_5^+$ in accordance with eq 9. Similarly, the

$$P_2H_5^+(PH_3)_{n-1} + PH_3 \rightleftharpoons P_2H_5^+(PH_3)_n \quad (9)$$

sequence of masses 99, 133, and 167 is observed, corresponding to the successive addition of $PH_3$ to $P_3H_6^+$, in accordance with reaction 10. Reaction 9 for ($n$ −

$$P_3H_6^+(PH_3)_{n-1} + PH_3 \rightleftharpoons P_3H_6^+(P_nH_3) \quad (10)$$

1), $n$ = 0 to 1, gave satisfactory equilibrium constants at several temperatures below 283°K, and thus the enthalpy and entropy of reaction were obtained. The addition of the second and third $PH_3$ molecule to $P_2H_5^+$, however, reached equilibrium only at 215°K and our equipment could not be operated satisfactorily at temperatures sufficiently below this to yield a satisfactory enthalpy of reaction. Thus, it was not possible to obtain the enthalpy and entropy of addition of the second and third $PH_3$ in reaction 9. The same considerations apply to reaction 10. The enthalpy and entropy of addition of one $PH_3$ to $P_3H_6$ were determined. Only the free energy of addition of the second $PH_3$ could be obtained, and there was not enough of the $(P_3H_6^+)(PH_3)_3$ formed to yield an equilibrium constant. The results are given in Tables III and IV. Although

**Table III.** Thermochemical Results for the Solvation of $P_2H_5^+$ (kcal/mol)

$$(P_2H_5^+)(PH_3)_{n-1} + PH_3 \rightleftharpoons P_2H_5^+(PH_3)_n$$

| $n-1, n$ | $T$°K | ln $K$ | $-\Delta G$ | $-\Delta H$ | $-\Delta S$, eu |
|---|---|---|---|---|---|
| 0, 1 | 233 | 9.6 | 4.5 | 9 | 19.3 |
| 0, 1 | 243 | 7.83 | 3.8 | 9 | 21.4 |
| 0, 1 | 257 | 7.22 | 3.7 | 9 | 20.6 |
| 0, 1 | 283 | 6.28 | 3.55 | 9 | 19.3 |
| 1, 2 | 215 | 8.5 | 3.66 | 9 | |
| 2, 3 | 215 | 7.8 | 3.33 | 9 | |

**Table IV.** Thermochemical Results for the Solvation of $C_3H_6^+$ (kcal/mol)

$$P_3H_6^+(PH_3)_{n-1} + PH_3 \rightleftharpoons P_3H_6^+(PH_3)_n$$

| $n-1, n$ | $T$°K | ln $K$ | $-\Delta G$ | $-\Delta H$ | $-\Delta S$, eu |
|---|---|---|---|---|---|
| 0, 1 | 205 | 9.45 | 3.88 | 10.8 | +34 |
| 0, 1 | 223 | 8.52 | 3.8 | 10.8 | +34 |
| 0, 1 | 233 | 6.11 | 2.85 | 10.8 | 34 |
| 0, 1 | 247 | 4.83 | 2.39 | 10.8 | 34 |
| 1, 2 | 215 | 7.61 | 3.27 | | |

they are less satisfactory than those of the $PH_4^+$ sequence, they are not unreasonable.

Because of the different temperatures at which the various solvation steps go to equilibrium, a direct comparison of the free energies of the solvation steps is not possible. However, the free energies of the various steps can be computed for 215°K where the second and third solvation steps of $P_2H_5^+$ and $P_3H_6^+$ were determined. Results so computed are given in Table V. It appears reasonable that the 0, 1 step for $P_3H_6^+$ should be compared to the 1, 2 step for $P_2H_5^+$ and the 2, 3 step for $PH_4^+$. Table V is arranged to show this comparison and it will be observed that the agreement is surprisingly good. The largest discrepancy is 0.7 kcal/mol and, while one could hope for closer

**Table V.** $-\Delta G_{215°K}$ (kcal/mol) for Comparable Solvation Steps for $PH_4^+$, $P_2H_5^+$, and $P_3H_6^+$

| | $(PH_4^+)$-$(PH_3)_{n-1,n}$ | $(P_2H_5^+)(PH_3)$ | $(P_3H_6^+)$-$(PH_3)_{n-1,n}$ |
|---|---|---|---|
| $n-1, n$ | 1, 2 | 0, 1 | |
| $-\Delta G$ | 4.4 | 3.7 | |
| $n-1, n$ | 2, 3 | 1, 2 | 0, 1 |
| $-\Delta G$ | 3.3 | 3.7 | 3.8 |
| $n-1, n$ | 3, 4 | 2, 3 | 1, 2 |
| $-\Delta G$ | 3.0 | 3.3 | 3.3 |

agreement, this is probably within the accuracy of our experiments.

## Discussion

**Kinetics.** At high temperatures, eq 1 can be treated

$$PH_4^+ + PH_3 \underset{k_{-1}}{\overset{k_1}{\rightleftharpoons}} (P_2H_7^+)^* \xrightarrow{k_2} P_2H_5^+ + H_2 \quad (1)$$

kinetically by the steady state approximation since $(P_2H_7^+)^*$ readily dissociates at high temperatures.

The rate of disappearance of $PH_4^+$ can be written as

$$-d[PH_4^+]/dt = k_1(PH_4^+)(PH_3) - k_{-1}(P_2H_7^+)^* \quad (11)$$

$$(P_2H_7^+)^* = k_1(PH_4^+)(PH_3)/(k_2 + k_{-1}) \quad (12)$$

Substituting (12) into (11) and integrating, we obtain

$$\ln (PH_4^+)/(PH_4^+)_0 = \frac{k_1k_2(PH_3)\tau}{k_{-1} + k_2} \quad (13)$$

In eq 13, one can substitute $\tau = C(PH_3)$, where $C$ is a constant calculated from the mobility equation for ion drift through a gas.[6]

By plotting ln $(PH_4^+)/(PH_4^+)_0$ against $(PH_3)^2C$, a line whose slope is $k_1k_2/(k_{-1} + k_2)$ is obtained. As the temperature is reduced, $k_{-1}$ becomes small and much less than $k_2$. Thus, in limit of low temperatures, this reduces to $k_1$. In this way, we found $k_1 = 3.8 \times 10^{-12}$ cm³/(molecule sec).

Reaction 1 is a collision reaction and can be expected to vary little with temperature over the range 0–160°. Combining $k_1$ with $K_{0,1}$, we compute $k_{-1}$ at various temperatures. From these results and the value of $k_1k_2/(k_{-1} + k_2)$ discussed above, we can compute $k_2$ at various temperatures.

The temperature dependence of $k_{-1}$ and $k_2$ can be expressed by means of Arrhenius equation

$$k = Ae - E_a/RT \quad (14)$$

The results obtained from the plot of log $k$ *vs.* $1/T$ for $k_{-1}$ and $k_2$ shown in Figures 8 and 9, respectively, are given in Table VI. From the slopes of the plots,

**Table VI.** Data from Arrhenius Plots ($k_1 = 3.8 \times 10^{-12}$ cm³/(molecule sec))

| | $A$, sec$^{-1}$ | $E_a$, kcal/mol |
|---|---|---|
| $k_{-1}$ | $9.4 \times 10^{12}$ | 10.7 |
| $k_2$ | $3.8 \times 10^{9}$ | 7.5 |

one can see at very low temperature $k_2$ is greater than $k_{-1}$ and the approximation used to calculate $k_1$ is valid.

(6) E. W. McDaniel, "Collision Phenomena in Ionized Gases," Wiley-Interscience, New York, N. Y., 1964, p 433.

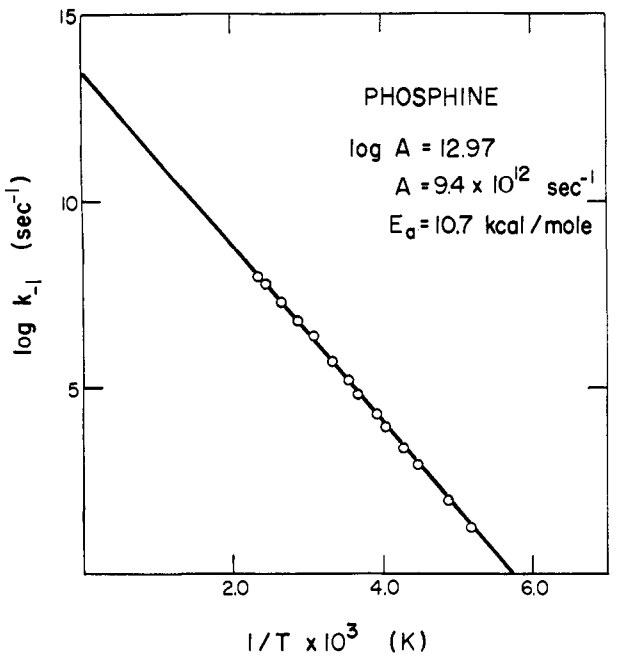


**Figure 8.** A plot of log $k_{-1}$ ($sec^{-1}$) *vs.* $1/T$ (°K). $k_1$ is the reverse dissociation rate constant in the reaction

$$PH_4^+ + PH_3 \underset{k_{-1}}{\overset{k_1}{\rightleftharpoons}} P_2H_7^+ \xrightarrow{k_2} P_2H_5^+ + H_2$$

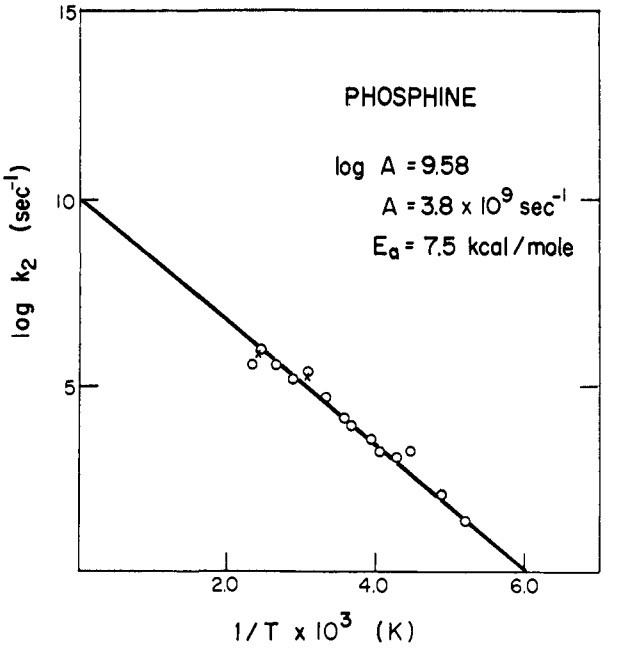


**Figure 9.** A plot of log $k_2$ ($sec^{-1}$) *vs.* $1/T$ (°K). $k_2$ is the forward dissociation rate constant in the reaction

$$PH_4^+ + PH_3 \underset{k_{-1}}{\overset{k_1}{\rightleftharpoons}} P_2H_7^+ \xrightarrow{k_2} P_2H_5^+ + H_2$$

Further, the activation energy of $k$ should equal the exothermic heat of the forward reaction. The discrepancy of only 0.8 kcal/mol is gratifying.

The results for the activation energy calculated from the rate constants agree quite well with those expected for a unimolecular dissociation process.

From reaction 1, we see

$$d[P_2H_5^+]/dt = k_2(P_2H_7^+)^* \quad (15)$$

$$(P_2H_5^+)/(PH_4^+)_0 = 1 - e - \frac{k_1k_2(PH_3)^2C}{k_2 + k_{-1}} \quad (16)$$

A plot of ln $[1 - (P_2H_5^+)/(PH_4^+)_0]$ *vs.* $(PH_3)^2C$ gives the same slope as eq 11. Using these data, $k_2$ at different temperatures were determined. The values calculated from the two equations were in good agreement.

**Estimations of Solvation Energies.** It is instructive to attempt to compute the potential energy of the stepwise addition of $PH_3$ to $PH_4^+$ and to compare the results to those of the $NH_4^+$–$NH_3$ system in an effort to ascertain the properties that determine the behavior of the two systems. Following Muirhead-Gould and Laidler[7] and Ďzidić and Kebarle,[8] we write

$$E_t = E_{dip} + E_{pol} + E_{dis} + R_{dip} + R_{el} \quad (17)$$

where $E_t$ is the total potential in a cluster of $PH_4^+$ with $n$$PH_3$ molecules and the remaining terms are as follows: $E_{dip}$, the ion–permanent dipole interaction, is given by $-e\mu_N/r^2$, where $e$ is the unit electric charge, $\mu_N$ is the dipole moment of $PH_3$, and $r$ is the P–P distance; $E_{pol}$, the ion–induced dipole interaction, is $-\alpha e^2/2r^4$, where $\alpha$ is the polarizability; $E_{dis}$, the van der Waals dispersion of ion–ligand and ligand–ligand interactions, is

$$-\frac{3}{2}\frac{\alpha_i\alpha_j}{(r_{ij})_6}\frac{I_iI_j}{I_i + I_j}$$

where $I$ is the ionization potential; $R_{dip}$ is the repulsion due to dipole–dipole and dipole–induced dipole interactions; $R_{el}$ is the electronic repulsions between the ion and ligand molecules. The values of the various parameters employed are given in Table VII.

**Table VII.** Parameters Employed in Computing Thermochemical Properties

| | |
|---|---|
| $PH_4^+$ | |
| $d$(P–H) | 1.42 Å |
| $r(PH_4^+)$ | 1.65 Å |
| $T_d$ | Symmetry |
| $\alpha$ | 2.5 $Å^3$ |
| $I$ | 10 eV, assumed |
| $PH_3$ | |
| $d$(P–H) | 1.42 Å |
| $r(PH_3)$ | 1.9 Å |
| ∠HPH | 93° |
| $\alpha$ (polarizability) | 4.27 $Å^3$ |
| $\mu_N$ | 0.55 D |
| $I$ | 10 eV |
| Dielectric constant, $K$ | 2.7 |
| $dK/dT$ | 0.0018 |
| $PH_4^+$–$PH_3$ | |
| $d(P^+$–P) | 2.95 Å |

We did not do the complete calculation of the various potential terms to minimize the potential energy functions and calculate the intermolecular distance between the $PH_4^+$ and $PH_3$.[8] Instead, this distance was estimated by correcting the sum of the $PH_4^+$ ionic radius

(7) J. S. Muirhead-Gould and K. J. Laidler, *Trans. Faraday Soc.*, **63**, 944, 953, 958 (1967).

(8) I. Dzidić and P. Kebarle, *J. Phys. Chem.*, **74**, 1466 (1970).

and the molecular radius of $PH_3$ for the shrinkage due to electrostatic forces. This shrinkage was found to be approximately 0.6 Å in the alkali ion–water system.[8] The ion–molecule distance for $PH_4^+$–$PH_3$ was estimated to be $r_{P-P}$ = 3.55 Å, which is probably a minimum distance.

In calculating the dipole contribution, we assumed 95% of the charge of this ion is found on the phosphorus atom since the electronegativity of phosphorus and hydrogen are equal.[9] This is, of course, an arbitrary assumption, since a greater portion of the charge may be distributed to the hydrogens. This would have the effect of reducing the net charge on the P atom of $PH_4^+$ and distributing a greater amount to the H atoms. This charge, however, while smaller, is also closer to the $PH_3$ molecule with the result that $E_{dip}$ and $E_{pol}$ are very little affected.

In computing the van der Waals dispersion, $r_{12}$ is the distance between the phosphorus atoms, $r_{P-P}$, plus the distance to the center of the phosphine molecule, 0.38 Å. For the ligand–ligand distance, $r_{12}$ is taken equal to the molecular diameter of phosphine. No value for the $PH_4^+$ ion polarizability exists, but from comparing ion to neutral polarizability for large atoms an estimate of one-half the neutral polarizability is used. The ionization potential of phosphine is 10.0 eV.[10] The same values for ionic and neutral polarizability of $PH_3$ are used in doing the $R_{dip}$ calculation. The distance of closest approach for ligand–ligand repulsion was taken as the distance between centers of four adjacent phosphine molecules tetrahedrally placed around the central ion.

The second repulsion term is the electronic cloud repulsion for the ion–ligand interaction.

$$R_{el} = A/r^{12} \quad (18)$$

One can estimate $A$ from available inert gas data by choosing an inert gas of similar size to the $PH_4^+$ ion.[8]

Gathering the terms, we obtain a qualitative estimate of the following electrostatic contributions (in kilocalories per mole) for the solvation of $PH_4^+$ by $PH_3$: $E_{dip}$, −4.4; $E_{pol}$, −7.4; $E_{dis}$, −1.3; $R_{dip}$, 0; $R_{el}$, 5; $E_t$, −8.1.

Several contributing factors are obvious even in this qualitative treatment of the electrostatic interactions. Thus, the total potential energy for the cluster formation is considerably less than that observed for the solvation of an ion of similar radius by a more highly polar molecule (see $Cs^+$ in ref 8). Since $E_{dis}$ and $R_{dip}$ are small, this decrease in energy of interaction is dependent on the magnitude of the ion–dipole, ion–induced dipole, and the electronic repulsion terms.

Unlike a highly polar system such as water or ammonia where the major contribution to the electrostatic interactions is the ion–dipole term, in phosphine this term is small because of the weak dipole (0.55 D) of phosphine and the ion–induced dipole predominates for the first solvation since the polarizability of phosphine is quite large (4.27 Å$^3$). However, since the second term is dependent on the $r^{-4}$ and the $R_{el}$ upon $r^{-12}$, these contributions rapidly drop off with ion–neutral distance. The combination of these physical factors explains the small values obtained for free energy and enthalpy of hydration. There is also general agreement between the magnitude of the solvation enthalpy and electrostatic potential energy for formation of the first solvated shell.

Considering the small solvation energies of phosphine for the primary solvation shell, $n$ = 0 to 4, it might be interesting to calculate the total energy of solvation for this ion in phosphine liquid and compare this result to that for ammonia.

The total heat of solvation of the $PH_4^+$ ion can be calculated from

$$\Delta H_{solv}(PH_4^+) = \Delta H_{0,n} + \Delta H_{solv}(PH_4^+ \cdot nPH_3) + n\Delta H_{vap}(PH_3) \quad (19)$$

$\Delta H_{0,n}$ is the enthalpy of producing the first solvation shell of $PH_3$ molecules. If we assign the first solvation shell as $n$ = 4 then $\Delta H_{0,4}(PH_4^+)$ = −34.2 kcal/mol from Table II. $\Delta H_{solv}(PH_4^+ \cdot 4PH_3)$ is the enthalpy of immersing $PH_4^+ \cdot 4PH_3$ in liquid $PH_3$ and can be calculated from the Born equation assuming the radius for the first solvation shell is $r_{shell} = r_{ion} + d_{NH_3}$.[11] We use $r_{PH_4^+}$ = 1.65 Å[12] and $d_{PH_3}$ = 3.89 Å;[13] therefore, $r_{shell} \simeq$ 5.5 Å.

The dielectric constant and change in dielectric constant with temperature are given by Palmer and Schmidt[14] as 2.7 and 0.0018, respectively. The resultant calculation gives $\Delta H_{solv}(PH_4^+ \cdot 4PH_3)$ = −27.5 kcal/mol. The heat of vaporization of phosphine is 3.5 kcal/mol giving $\Delta H_{solv}(PH_4^+)$ = −47.7 kcal/mol.

Using a similar cycle, one can calculate the heat of solvation of the ammonium ion in ammonia $\Delta H_{solv}(NH_4^+)$ = −90 kcal/mol.[15] Again, the fact that phosphine has a weak dipole manifests itself in the low heat of phosphination of the $PH_4^+$ ion. The low-solvation value for phosphine suggests the solution phase has no strong structural features such as are present in the hydrogen-bonded systems of ammonia and water. The phosphine and ammonia results are compared in Table VIII.

**Table VIII.** Comparison of Thermochemical Values for Stepwise Addition of Solvent to Ion in Phosphine and Ammonia

| | −ΔH, kcal/mol | | −ΔS, eu | |
|---|---|---|---|---|
| $n-1, n$ | $PH_4^+$–$PH_3$ | $NH_4^+$–$NH_3$ | $PH_4^+$–$PH_3$ | $NH_4^+$–$NH_3$ |
| 0, 1 | 11.5 | 27 | 25.9 | 32 |
| 1, 2 | 9.2 | 17 | 22.3 | 26.8 |
| 2, 3 | 7.3 | 16.5 | 18.4 | 34 |
| 3, 4 | 6.2 | 14.5 | 15 | 36 |
| 4, 5 | 5.5 | 7.5 | 13.2 | 25 |

We can see that the small free energy and enthalpy values observed in Table II do reflect the weak interactions of a large ion with a nearly nonpolar solvent.

Turning now to the entropy term, the magnitude observed for the first solvation is similar to that observed

(9) L. Pauling, "The Nature of the Chemical Bond," 3rd ed, Cornell University Press, Ithaca, N. Y., 1960.

(10) J. D. Morrison and J. C. Traeger, *Int. J. Mass Spectrom. Ion Phys.*, 11, 277 (1973).

(11) (a) M. Born, *Z. Physik*, 1, 45 (1920); (b) see F. Basolo and R. G. Pearson, "Mechanisms of Inorganic Reactions," Wiley, New York, N. Y., 1968.

(12) H. F. Halliwell and S. C. Nyberg, *Trans. Faraday Soc.*, 59, 1129 (1963).

(13) S. M. Vlasov and G. G. Devyatykh, *Zh. Neorg. Khim.*, 11 (12), 2681 (1966).

(14) R. C. Palmer and H. Schmidt, *J. Phys. Chem.*, 15, 381 (1911).

(15) P. Kebarle, *Advan. Chem. Ser.*, No. 72, 24 (1968).

for other large ion systems.[16] The entropy for the addition of the first phosphine to $PH_4^+$ can be calculated. The translational entropy change is calculated from the Sackur–Tetrode equation $\Delta S_{trans} = -34.5$ eu. The rotational entropy can be calculated[17] from the equation

$$\Delta S_{rot} = {}^1/_2 R \ln (I_A I_B I_C)_2/(I_A I_B I_C)_1 = 6.4 \text{ eu} \quad (20)$$

The vibrational entropy can be estimated from the six new modes of vibration in the $PH_4^+ \cdot PH_3$ complex. One would expect one new stretching frequency of the P–P bond formed and two bending frequencies of the P–$PH_3$ bond. The three additional modes would be either deformation of hydrogen rocking. To approximate the magnitude of these frequencies, we use the spectroscopic results for diphosphine.[18] The stretching frequency for the P–P bond in this compound is $\nu_s' \sim 450$ cm$^{-1}$ and the bending frequency $\nu_b' \sim 400$ cm$^{-1}$. The remaining three modes would be expected to have frequencies of at least 800 cm$^{-1}$ and at the temperature of these studies would make no significant contribution to the entropy. From Benson's correlation table for vibration entropy and frequency,[19] we estimate the $\Delta S_{vib} \sim 3$ eu. The calculated total entropy change is $\Delta S_{total} = -25.1$ eu. This is in good agreement with the observed $\Delta S_{0,1} = -25.9$ eu.

(16) P. Kebarle in "Ion-Molecule Reactions," Vol. 1, J. L. Franklin, Ed., Plenum Press, New York, N. Y., 1972, Chapter 7.

(17) The moments of inertia of phosphine are known from spectroscopic data: $I_A = 7.16$, $I_B = I_C = 6.29 \times 10^{-40}$ g cm$^2$: C. A. Burrus, Jr., A. Jache, and W. Gordy, *Phys. Rev.*, **95**, 706 (1954); A. P. Altshuller, *J. Amer. Chem. Soc.*, 77, 4220 (1955). The moments of inertia for $PH_4^+ \cdot PH_3$ can be calculated using a symmetrical top model for the complex (E. A. Moelwyn-Hughes, "Physical Chemistry," Pergamon Press, London, 1957, p 496): $I_A = 7.16 \times 10^{-40}$ g cm$^2$, $I_B = I_C = 160 \times 10^{-40}$ g cm$^2$.

(18) (a) M. Baudler and L. Schmidt, *Z. Anorg. Allg. Chem.*, **289**, 219 (1957); (b) see D. E. C. Corbridge, "Topics in Phosphorus Chemistry," Vol. 6, M. Grayson and E. J. Griffith, Ed., Interscience, New York, N. Y., 1969, p 235.

(19) S. W. Benson, "Thermochemical Kinetics," Wiley, New York, N. Y., 1968.

There is a constant decrease in entropy with successive solvation steps as shown in Table I. This trend suggests a very loose complex is formed as larger numbers of $PH_3$ molecules are joined to the central ion. From the electrostatic considerations, this is what one might expect. Since the diameter of the phosphine neutral is quite large and the electrostatic bonding forces small, the entropy change with solvation decreases as molecules are bound further away from the central ion. This result is in contrast to the ammonia results where no decrease in entropy is observed within the first solvation shell.[16]

## Conclusion

The ion–solvent reactions of phosphine with its major product ions are reported. These reactions have not been observed previously. A study of the equilibrium constants for the solvation of $PH_4^+$ gives thermochemical values for the solvation of a large ion in a nonpolar gas. A better understanding of the contributions the neutral gas makes to the total interaction potential of ion solvation in the gas phase is obtained by studying the difference in thermochemical data between phosphine and ammonia. The differences in these results reflect the increase in solvation efficiency of a small polar molecule over a large nonpolar one. From the total solvation energies calculated for the two congeners, one can see that a major contribution to the total solvation energy of any ion is the energy required to form the first solvation shell. Hopefully, future work with different ions in both polar and nonpolar solvent gases may shed further light on the individual energy contributions to the total ion-solvation energy in both the gas phase and the solution phase.

**Acknowledgment.** The authors wish to express their appreciation for the support of The Robert A. Welch Foundation.

# Conformational Analysis of Some Fluoro Alcohols. CNDO/2 Calculations, Infrared Evidence, and Dipole Moments[1]

**D. R. Truax,* H. Wieser, P. N. Lewis,[2] and R. S. Roche**

*Contribution from the Chemistry Department, University of Calgary, Calgary, Alberta, Canada T2N 1N4.* *Received August 1, 1973*

**Abstract:** A conformational analysis was carried out on hexafluoropropan-2,2-diol, fluoral hydrate, and hexafluoropropan-2-ol using the semiempirical CNDO/2 method. The more stable structures found for these molecules conform to those predicted from the dominance of one, or some combination of the gauche effect, trans lone-pair effect and intramolecular hydrogen bonding. The results are shown to be consistent with the experimental dipole moments and infrared evidence.

Since the earliest observations of splitting and asymmetry of the infrared bands associated with the hydroxyl stretching mode in alcohols, it has been recognized that rotational isomerism about the CO bond is the origin of the observed effects.[3-5] With the development of *ab initio* and semiempirical molecular orbital methods for the calculation of the potential energy of a molecule as a function of molecular geom-

(1) Contribution No. 73-02 from the Biopolymer Research Group, University of Calgary.

(2) Biophysics Laboratories, Portsmouth Polytechnic, Portsmouth, England.

(3) R. M. Badger and S. H. Bauer, *J. Chem. Phys.*, 4, 711 (1936).

(4) R. Piccolini and S. Winstein, *Tetrahedron Lett.*, 4 (1959).

(5) F. Dalton, G. P. Meakins, J. H. Robinson, and W. Zaharia, *J. Chem. Soc.*, 1566 (1962).